

Linear Stability Analysis of DBD Boundary-Layer Flow-Control Experiments and Simulations

Alexander Duchmann^{1*}, Cameron Tropea^{1,2}, and Sven Grundmann¹

¹Center of Smart Interfaces, Technische Universität Darmstadt,
Flughafenstr. 19, D-64347 Griesheim, Germany

²Institute of Fluid Mechanics and Aerodynamics, Technische Universität Darmstadt,
Flughafenstr. 19, D-64347 Griesheim, Germany

Received date 4/17/2013; Accepted date 7/5/2013

Abstract

Linear stability theory is applied to analyze boundary-layer data from flow-control experiments with dielectric barrier discharge plasma actuators. The hydrodynamic stability of laminar boundary-layer flow along a flat plate subject to an adverse pressure gradient is enhanced by the induced momentum from a dielectric barrier discharge. Changes in the velocity distribution are measured with laser Doppler anemometry while a traversable hot-wire probe quantifies the macroscopic effect on the transition location. The observed connection between the altered velocity distribution and the delayed transition is supported by a stability analysis of experimental boundary-layer profiles. A numerical procedure to study the impact plasma actuation has on hydrodynamic stability is presented to enable parametric studies and optimization of flow-control applications.

1. INTRODUCTION

The influence of dielectric barrier discharges (DBD) on boundary-layer transition has been investigated in numerous wind tunnel experiments and numerical studies. Several researchers observed an acceleration of boundary-layer transition [1,2] whereas others published results of delayed transition [3,4]. Computational investigations [5] and stability considerations [6,7] indicate that the additional momentum fed into a laminar boundary layer subtly changes the mean velocity profiles; hence reducing the susceptibility towards Tollmien-Schlichting instabilities. The DBD actuation dampens existing flow instabilities which are otherwise amplified and eventually initiate the breakdown to turbulence. Thus, the breakdown to the turbulent state can be delayed and a net reduction of skin friction drag is achieved.

Despite the successful application of DBD for transition delay in Tollmien-Schlichting dominated boundary-layer flow, only few investigations concentrate on explaining the effect by means of hydrodynamic stability analysis. Duchmann et al. [6] conducted a linear stability analysis in the spatial framework for boundary-layer data from large eddy simulations (LES) by Quadros [5]. A prominent effect on the critical Reynolds number and reduction of the disturbance growth rates within the stabilized velocity field are reported. Additionally, experimental data derived from hot-wire measurements were analyzed yielding qualitative agreement with the numerical results. More recently, a stability analysis was performed for direct numerical simulations (DNS) of a laminar boundary-layer flow subjected to DBD forcing [8]. Both investigations demonstrate the applicability of linear stability theory to the flow control with DBD actuators. Rihard and Roy [7] analyzed a generic flow composed of a Blasius boundary layer superimposed onto a Glauert wall jet in an attempt to mimic the effect of a DBD device. Although this linear superposition does not necessarily satisfy the Navier-Stokes equations, the results from linear stability analysis in the temporal framework indicate that excessive control can provoke inviscid instabilities due to non-monotonic curvature of the velocity profile.

The shortcomings of earlier investigations motivate the present study, with the aim of analyzing experimentally measured velocity profiles under the influence of DBD actuation in terms of hydrodynamic stability. Since the zone of ionization next to the exposed electrode is not accessible by intrusive probes, only optical measurement techniques enable a close-up view of the flow manipulation.

*corresponding author: duchmann@csi.tu-darmstadt.de

A laser Doppler anemometer (LDA) is chosen to resolve the averaged streamwise and wall-normal velocity components of the boundary-layer flow. Measurement uncertainties complicate the analysis based on first and second derivatives of the boundary-layer velocity profiles with respect to the wall-normal coordinate, but adequate filtering and averaging permits the processing of such data with the stability code.

More conveniently, a numerical study of the flow-control effect can be performed. A finite-difference solver for the solution of laminar boundary-layer equations is presented, incorporating a plasma force model experimentally measured by Kriegseis *et al.* [9]. The numerical routine enables a systematic variation of parameters to find optimized flow-control configurations.

2. LINEAR STABILITY ANALYSIS

In order to investigate the plasma actuator's influence on flow stability, modal linear stability analysis is conducted. The local manipulation of the boundary-layer profiles by the plasma actuator reduces the flow's affinity to become unstable in the presence of two-dimensional Tollmien-Schlichting instabilities. The linear stability analysis performed in the present work assumes low environmental disturbances and a parallel, two-dimensional, steady base flow U , which is superimposed with small wavelike disturbances u' and p' . A system of two linear disturbance equations for the wall-normal velocity component v' and the wall-normal vorticity component Ω' is sufficient to describe the evolution of the modal instabilities. The initial growth of the small disturbances may be described by the wave modes v' and Ω' . The resulting Orr-Sommerfeld and Squire equations

$$\begin{aligned} \left[(-i\omega + i\alpha U)(\mathcal{D}^2 - k^2) - i\alpha \frac{d^2U}{dy^2} - \frac{1}{\text{Re}}(\mathcal{D}^2 - k^2)^2 \right] \hat{v} &= 0 \\ \left[-i\omega + i\alpha U - \frac{1}{\text{Re}}(\mathcal{D}^2 - k^2) \right] \hat{\Omega} &= -i\beta \frac{dU}{dy} \hat{v} \end{aligned}$$

with $\mathcal{D} = \frac{\partial}{\partial y}$ pose a boundary-value problem with homogeneous boundary conditions at the wall and in the free stream. The problem is defined in dependence of a spatial disturbance wave number $k = (\alpha^2 + \beta^2)^{0.5}$ and a temporal disturbance frequency ω . The resulting equations for the disturbance behavior in time and space can only be solved numerically.

In the present work the numerical problem is solved for the spatial framework, providing a given disturbance frequency ω and solving for the complex streamwise wave number $\alpha = \alpha_r + i \alpha_i$. The spanwise wave number β is zero for the assumption of plane two-dimensional waves. The spatial approach is appropriate to describe the downstream evolution of such instabilities in the linear amplification stage. To reduce the nonlinear eigenvalue problem to a linear one, two consecutive transformations are necessary, an exponential variable transformation and a companion matrix method. In order to discretize the boundary-value problem for a numerical solution, a spectral Chebyshev collocation method is chosen. The dependent variables v and Ω are represented by truncated sums of Chebyshev polynomials and a Gauss-Lobatto grid is used for the discrete representation of the independent variable y . Since the Gauss-Lobatto points are only defined on the finite domain $\xi = [-1, 1]$ the algebraic function $y(\xi) = \delta/2 (1 + \xi)$ maps the grid points into the physical boundary-layer domain $y = [0, \delta]$. Typically, the boundary-layer profiles are resolved by 80 grid points with increased resolution close to the solid surface. The resulting discretized matrix equations are solved with a built-in routine in *MATLAB*.

3. EXPERIMENTAL SETUP

Boundary-layer profiles subjected to DBD forcing have been obtained from hot-wire measurements and analyzed with a linear stability code by Duchmann *et al.* [6], showing good agreement with numerical data. Due to a minimum distance of the hot-wire probe from the actuator, the velocity profiles in its direct proximity could not be measured. Since the highest impact on the flow stability is expected in this area, laser optical measurements accessing the zone of ionization are necessary.

An open-circuit wind tunnel with a 1:24 contraction nozzle is operated at a nominal free-stream velocity of $U = 20\text{m/s}$ for the flow-control experiments reported hereafter. An average turbulence intensity of $Tu = 0.24\%$ is measured at the inlet of the 450mm x 450mm test section, containing a flat

plate of 1600mm length with an 1:6 elliptical leading edge. The trailing edge angle is adjustable for accurate positioning of the stagnation point, intended to mitigate boundary-layer separation next to the leading edge. The flat plate provides an insert to flush mount a dielectric barrier discharge actuator 350mm downstream of the leading edge. A 900mm long displacement body is installed on the tunnel upper wall to destabilize the laminar boundary-layer flow and provoke accelerated growth of Tollmien-Schlichting instabilities. The maximum thickness of the displacement body is located at the beginning of the flat plate, creating an almost constant adverse pressure gradient of 83.6Pa/m downstream of the leading edge. The experimental setup with a single DBD actuator at $x_{DBD}=350\text{mm}$ is illustrated in Figure 1 and can be reviewed in more detail in [10, 11].

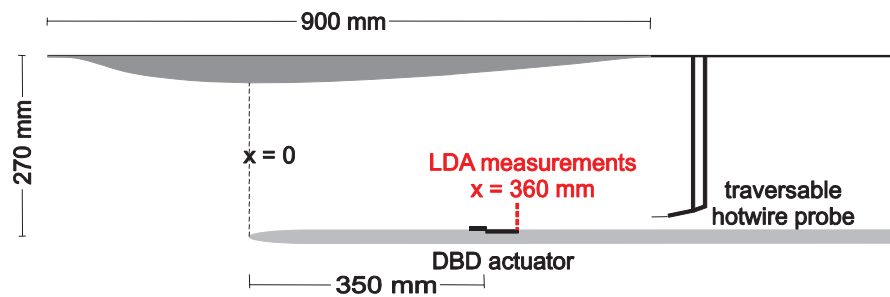


Figure 1: Experimental setup within wind tunnel test section.

The streamwise and wall-normal velocity distribution next to the DBD actuator is measured with a *Dantec* two-velocity component LDA system with 300mm focal length, mounted on a *ISEL* 3D-traverse system. The laminar boundary-layer flow with and without DBD actuation can be compared and analyzed with the linear stability solver presented in Section 2. A single hot-wire probe connected to a *DISA* M-series constant temperature anemometer (CTA) can be positioned by a *Velmex* 2D-traverse between $x = 400\text{-}800\text{mm}$ and $y = 0\text{-}200\text{mm}$ along the center plane of the flat plate. The hot-wire data is used to measure transitional boundary-layer profiles and quantify the transition location. The CTA measurements enable a Fourier analysis of the frequency content within the boundary-layer, enabling detection of the unstable Tollmien-Schlichting modes, which turn out to be amplified in a frequency band between 200 and 400Hz.

The DBD actuator used in the present study is flush-mounted at $x_{DBD} = 350\text{mm}$ downstream of the leading edge. It consists of two copper electrodes separated by 0.3mm thick Kapton, forming the dielectric barrier. Copper tape of 0.035mm thickness constitutes the exposed and embedded electrode with a streamwise width of 2.5mm and 10mm, respectively. A *GBS Elektronik* MiniPuls 2.1 supplies the sinusoidal high voltage necessary for the discharge generation, enabling operation with an effective power consumption P between 45.7 and 64.4W per meter actuator length. The actuator length in the spanwise dimension is 440mm in the present case, spanning the whole width of the wind tunnel test section. The well-established actuator setup [3,9,10,17,18] ensures an uniform glow discharge without filaments, providing a two-dimensional flow-control force in streamwise direction.

Kriegseis *et al.* [9] identified the spatial force distribution of a single DBD actuator by PIV measurements in quiescent air. Such a force distribution can be implemented in numerical codes to calculate the effect on boundary-layer flow, as demonstrated in Section 5. Exemplarily, the spatial distribution of the streamwise force component is illustrated in Figure 2. Additionally, force balance measurements are available to quantify the thrust imposed on the fluid via a direct measurement method. A correlation between the power consumption P and the produced thrust T reveals a monotonic dependence. For a unique plasma actuator configuration, experimentally easily accessible power measurements can be directly related to the integral thrust imposed on the fluid, which is a prerequisite to relate experimental data to numerical simulations with a given force distribution. In order to maintain consistency with Kriegseis [12] both the integral thrust value, as well as the power consumption will always be quoted.

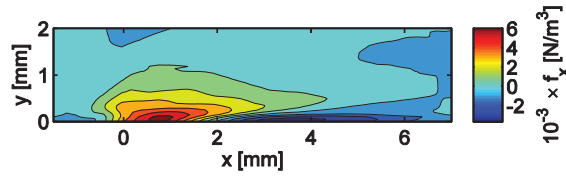


Figure 2: Spatial distribution of streamwise DBD force component.

4. EXPERIMENTAL RESULTS

Hot-wire measurements along the flat plate at a constant distance to the surface ($y = 1\text{mm}$) reveal the fluctuation of the velocity signal associated with boundary-layer transition. The root-mean-square value of the signal can be used as an indicator for the state of the boundary layer. Initially, the laminar boundary layer exhibits low fluctuations, indicated for the case without flow control (solid line) in Figure 3 (a) for $x < 450\text{mm}$. As the transition to turbulence is initiated, the flow becomes intermittent, constantly changing between the laminar and turbulent state due to the random occurrence of turbulent spots. In this region, the standard deviation of the velocity signal culminates indicating the point of maximum intermittency which will henceforth be arbitrarily defined as the ‘transition location’ x_{trans} . Further downstream, the fully turbulent flow has a higher variance than the laminar one, but due to the homogeneously distributed turbulence the standard deviation remains lower than in the intermittent region.

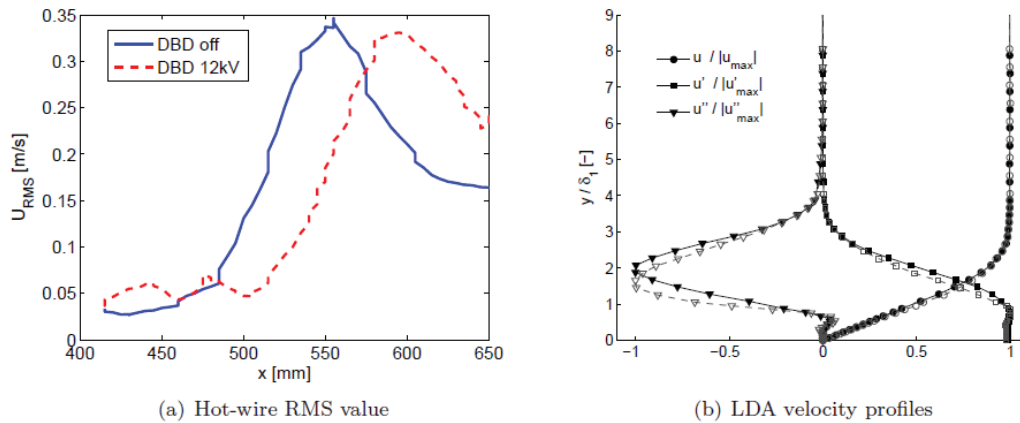


Figure 3: Experimental Quantification of transition location (a) and local boundary-layer manipulation (b).

For the described experimental setup, the transition location for a velocity of $U = 20\text{m/s}$ without DBD actuation is found at approximately $x_{trans,off} = 555\text{mm}$, corresponding to a Reynolds number $Re_x = 730.000$. If the single DBD actuator is powered at $P = 55.1\text{W/m}$, producing a net thrust of $T = 13.5\text{mN/m}$, the transition location is postponed to $x_{trans,on} = 595\text{mm}$ as indicated in Figure 3 (a). This transition delay of $\Delta x_{trans} = 40\text{mm}$ or 7.2% Reynolds number represents an average value for flat plate transition control, and is not the maximum which can be achieved by optimized operation. Nevertheless, this setting is useful for the investigation of the stability properties of the flow.

Two-velocity component LDA enables highly resolved pointwise flow measurements of two perpendicular velocity components. In the present work the streamwise and the wall-normal velocities u and v within the boundary-layer flow are acquired. The small interferometric sensor volume, in combination with the transparent acrylic surface of the flat plate, avoids reflections and enables accurate velocity measurements close to the surface. This is of importance for the determination of the exact wall distance and profile curvature, enabling sufficiently accurate analysis of the viscous flow stability. LDA measurements 10mm downstream of the exposed actuator electrode show the added momentum due to local flow acceleration. Figure 3 (b) illustrates the averaged velocity profiles $u(y)$ (circles), the first derivative $u'(y)$ (squares) and the second derivative $u''(y)$ (triangles) with respect to the normalized wall normal coordinate y/δ_1 at $x = 360\text{mm}$. The normalization of the wall-normal

coordinate is achieved by introducing the displacement thickness δ_l , an integral value resembling the boundary-layer profile shape. The values are normalized with the respective maximum to facilitate combination of all quantities in one graph. Filled symbols illustrate the baseline case whereas empty symbols represent DBD actuation at a thrust of $T = 13.5\text{mN/m}$, or the corresponding power consumption of $P = 55.1\text{W/m}$. A difference between the averaged profiles with and without DBD operation is hardly visible, but especially the second derivative shows a significant deviation at this position 10mm downstream of the exposed electrode. The second derivative indicates the profile curvature which appears in the Orr-Sommerfeld equation, indicating its major importance for the flow stability. A small alteration of the velocity profile and its curvature can have a significant impact on the flow stability and the transition process.

The acquisition of such accurate boundary-layer data is difficult and time consuming and should be limited to the region where an impact of DBD forcing on the velocity profiles is expected. The finely resolved data is analyzed with the linear stability solver described in Section 2. The DBD actuator at $x_{DBD}=350\text{mm}$ is operated at various thrust levels and the laser Doppler anemometry provides the averaged velocity profiles and relevant derivatives 10mm downstream, as exemplarily illustrated in Figure 3 (b). The experimental data is converted into an adequate format by scaling the velocity with the freestream speed and the wall-normal distance with the Blasius length scale, $\delta_N = (Re_x U_\ell/x)^{0.5}$. The normalization employs a dependence on the current streamwise flow position through the local Reynolds number Re_x as well as the flow velocity at the edge of the boundary layer, U_ℓ . Subsequently, the normalized profile is projected in the streamwise dimension by varying the local Reynolds number within the Blasius length scale. This corresponds to an assumption of self-similarity and an analytical variation of the local Reynolds number for the given profile. It is important to note that the following considerations are of theoretical nature, since a constant boundary-layer shape along the streamwise direction is assumed, only increasing the boundary-layer thickness according to theoretical scaling laws. In reality, the velocity profile is modified only within a short distance downstream of the actuator. The following considerations can be understood as an approximation of a boundary-layer flow under the influence of repeated actuation, e.g. by an array of plasma actuators. The theoretical amplification of disturbances along the streamwise direction can then be calculated with the linear stability code. The impact of DBD thrust variations is quantified by the growth rate of single disturbance frequencies or in terms of the critical Reynolds number, both approaches being visualized in Figure 4.

Figure 4 (a) portrays the predicted N -factor [13] evolution of a modal instability at $f = 200\text{Hz}$ under a variation of the actuator thrust. The N -factor is a measure of the integral disturbance amplification. It represents the local disturbance amplitude normalized with the initial amplitude at the initiation of disturbance growth at the critical point x_{cr} . Without DBD operation, the flow under the effect of an adverse pressure gradient becomes unstable at $x = 0.2\text{m}$, leading to increasing N -factors throughout the remaining flow domain. If the DBD actuator is operated, attenuation of the growth rates with increasing actuator thrust is observed. This also agrees with expectations, since the DBD actuation 10mm upstream enhances the flow stability and leads to a delayed transition, quantified by hot-wire measurements in Figure 3 (a).

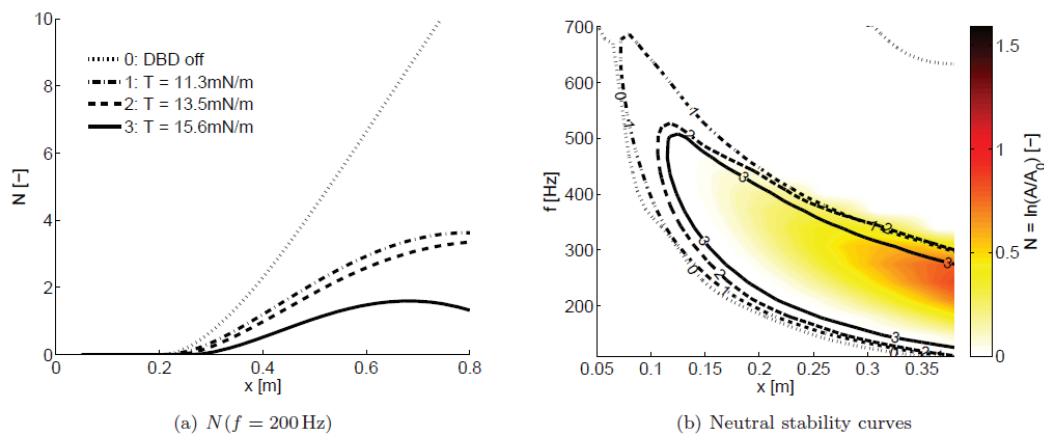


Figure 4: N -factor evolution of 200Hz disturbance frequency (a) and neutral stability curves (b) for DBD thrust variation between $T = 11.3 - 15.6\text{mN/m}$ ($P = 45.7 - 64.4\text{W/m}$).

Since transition is not initiated by a single frequency disturbance, the analysis of the neutral stability curve is more convenient. Based on the similarity approach in streamwise direction, a global influence on the stability is projected. Figure 4 (b) contains the neutral stability curves for the same DBD thrust levels with the same line styles and numbering as in (a). The color levels additionally illustrate the N -factor evolution for the highest thrust case 3. The four neutral stability curves show increasing values of the critical point x_{cr} and shrinking instability regions with increasing actuator thrust. Whereas the critical point is hardly distinguishable without DBD operation, it can be found at $x = 0.072\text{m}$ for $T_1 = 11.3\text{mN/m}$ ($P = 45.7\text{W/m}$). At the maximum thrust level $T_3 = 15.6\text{mN/m}$ ($P = 64.4\text{W/m}$), it is delayed until $x = 0.117\text{m}$, which corresponds to an increase by 62% compared to the minimum thrust value.

To enable a stability analysis at various locations and to avoid the self-similar scaling approach, fine resolution is required not only of the wall-normal, but also of the streamwise direction. Such measurements are time consuming, but would surely help to further quantify the stabilization impact and its gradient in the streamwise direction close to the DBD force field. For a less time consuming investigation of the stability impact, a numerical procedure is required. Such a computational tool enables extensive parameter variations, e.g. various actuator geometries, positions and thrust magnitudes. Even more importantly, the effect of multiple actuators arrays lined up in streamwise direction can be simulated. This can be a way to enhance the flow-control effectiveness, which is beyond the scope of experimental studies since the actuator location cannot be easily changed without deteriorating the surface smoothness of the experimental setup.

5. NUMERICAL INVESTIGATIONS

One possible numerical approach to study the effect of DBD operation on boundary-layer transition are direct numerical simulations (DNS), eventually including the full transition process. For practical applications at elevated Reynolds numbers, computational costs are prohibitive. A simplified model is required to compute the boundary-layer development on various flow geometries, e.g. flat plates or airfoils under the influence of DBD forcing. Köhler [14] successfully implemented a finite-difference scheme for the approximation of the laminar boundary layer along flat plates and natural laminar flow (NLF) airfoils within the *MATLAB* computing environment. The approach is based on the Falkner-Skan transformation of boundary-layer profiles and employs a solution procedure according to Cebeci and Keller [15] for the two-dimensional, incompressible and steady boundary-layer equations. A representation of laminar boundary-layer flow can be obtained, provided that a pressure distribution is externally supplied. Experimental pressure measurements as well as simple potential-flow solvers can provide the pressure gradient in streamwise direction to initiate the boundary-layer computations. The resulting flow field can be coupled to the linear stability analysis presented in Section 2. The combination of the numerical schemes is capable of accurately evaluating the influence of DBD actuation on the stability properties of laminar boundary-layer flow.

The missing link between the stability computations and a representation of the flow-control effect within the finite-difference boundary-layer code is an appropriate model of the DBD force field. Several phenomenological models exist to approximate the spatial distribution of the applied volume force [16-18], but most of them do not correctly describe the local introduction of momentum to the surrounding fluid. Maden *et al.* [19] observed significant differences for the case of induced wall-tangential flow in quiescent air, dependent on the chosen force representation. Such differences largely influence the outcome of a local stability analysis since the fluid velocity distribution and the stability properties may not be correctly represented. The only acceptable model for application with stability computations, which are highly susceptible to local gradients, is a distribution derived from experimental data by Kriegseis *et al.* [9]. The model resolves the wall-normal and the streamwise force component, confirming the prominence of the latter for the flow-control effect. For implementation of the force in the numerical study, the finely resolved spatial force distribution is interpolated onto the numerical grid and normalized with the applicable fluid density and the Blasius reference length scale, $F^* = F / (\rho \delta_N^2)$, asterisks indicating dimensional values.

The boundary-layer code in connection with the implemented force model, allows the calculation of laminar boundary-layer velocity profiles along arbitrary bodies. To predict and optimize the effectiveness of DBD transition control applied to the flight setup presented by Duchmann *et al.* [20], a computational study is performed. The panel-based *XFoil* [21] is used to calculate the pressure distribution for the NLF airfoil that constitutes the measurement wing glove used in the cited study. Successful in-flight transition delay is reported for an angle of attack of $\alpha = 0.7^\circ$ and a flow speed of

$U = 38\text{m/s}$, initializing the boundary-layer computations with the observed quasi-linear pressure gradient along the suction side of the airfoil. The resulting laminar boundary-layer flow field is subjected to stability analysis to enable a correlation between the computed N -factor evolution and the experimentally measured transition location.

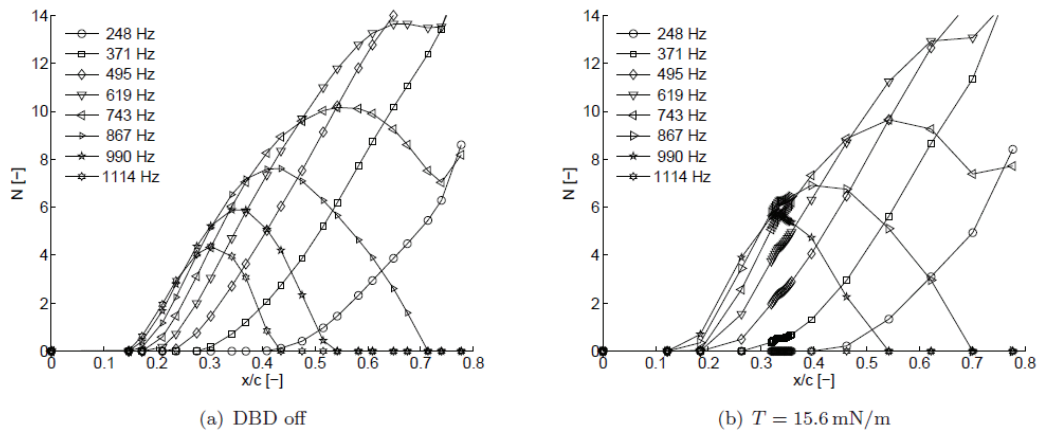


Figure 5: N -factor evolution of discrete disturbance frequencies (a) without and (b) with DBD thrust $T = 15.6\text{mN/m}$ ($P = 66.6\text{W/m}$).

The N -factor evolution of discrete disturbance frequencies is illustrated in Figure 5 (a) without DBD forcing. The experimentally observed transition location without DBD actuation, $x/c = 0.48$, corresponds to a critical N -factor threshold value of $N_t = 10$ which is in agreement with other flight experiments, as reviewed by Arnal *et al.* [22]. This value is used to numerically predict the transition location under the effect of a single DBD actuator positioned at $x/c=0.33$ on the pressure side of the wing glove airfoil. The actuator force field for a thrust of $T = 15.6\text{mN/m}$ is incorporated in the boundary-layer computation. This actuator thrust level approximately corresponds to in-flight operation under flow-control conditions at a power consumption of $P = 66.6\text{W/m}$. The boundary-layer profiles are locally influenced, and so are the stability properties. Figure 5 (b) indicates a local decrease of the N -factor evolution for all illustrated frequencies. Please note that the illustrated markers are clustered close to the actuator position due to a local refinement of the numerical grid to accurately resolve the actuator effect. The critical threshold $N_t=10$ is crossed at $x/c = 0.5$, which yields a predicted transition delay of $\Delta x_{trans}/c = 2\%$. This numerical prediction slightly underestimates the experimentally measured effect of 3%. It can therefore be expected that the chosen numerical procedure will provide a conservative estimate for the flow-control success.

Since the actuator force field can be arbitrarily simulated along the surface of any investigated body in numerical studies, the sensitivity of the flow stability to a variation of the actuator location can be easily evaluated. Such parametric studies are not feasible experimentally because of the elaborate model adjustments required for each case. Nevertheless, it is expected that a variation of the actuator position and a streamwise cascade of several actuators can significantly improve the flow-control effect. DNS computations by Vieira *et al.* [23] indicate increased effectiveness of multiple actuators for TS-wave attenuation within their linear evolution regime. Whereas a second actuator significantly reduces the absolute amplitudes, a third actuator does not add supplementary benefit for Blasius flat plate flow at $U = 10\text{m/s}$ in the absence of a pressure gradient. This diminishing marginal utility renders large actuator arrays unappealing unless a complete suppression of the disturbance growth can be attained along the surface.

The effect of large actuator arrays at very low thrust with minimized power consumption is simulated with the boundary-layer code and analyzed based on linear stability theory. The results of distributed DBD forcing on the generic flat plate setup presented in Section 3 at $U = 20\text{m/s}$ are presented in Figure 6. Twenty-six DBD actuators between $x = 0.33\text{-}0.58\text{m}$ are simulated with 10mm streamwise spacing to operate at a minimal thrust level of $T = 7.8\text{mN/m}$ ($P = 33.7\text{W/m}$).

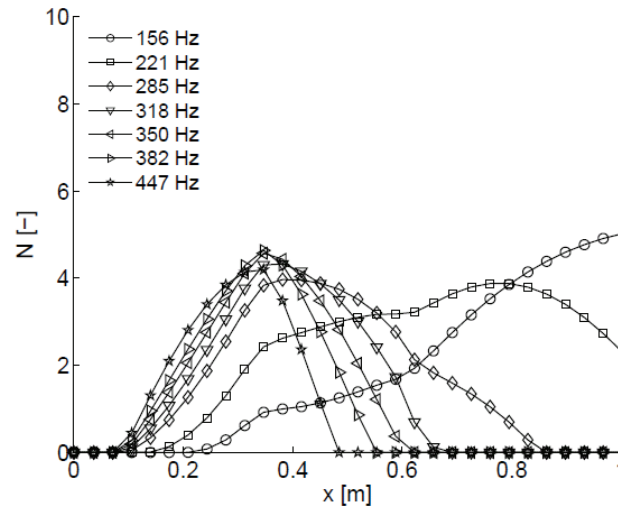


Figure 6: Theoretical N -factor evolution under distributed DBD forcing between $x = 0.33\text{m}$ and 0.58m at minimum thrust $T = 7.8\text{mN/m}$ ($P = 33.7\text{W/m}$).

Downstream of the first actuator location, the resulting N -factor evolution shows almost complete suppression of the wave amplitude over a large frequency range and attenuation to subcritical values for frequencies above 200Hz. Such a configuration is presently not feasible in experiments due to spacing limitations imposed by the electric potential differences, but specialized future DBD actuators may enable spatially continuous thrust generation. In the hypothetical case of infinitesimal distance between single actuators, a continuous acceleration of the fluid is possible and leads to the complete suppression of two-dimensional instabilities. Such a flow-control impact can be compared to continuous boundary-layer suction, yielding very stable flow conditions [24].

Although the effectiveness of flow control can be significantly enhanced by increasing the number of actuators and the total force magnitude, the energetic efficiency should be considered. A limited number of adequately positioned DBD actuators may provide an optimum in terms of the flow-control efficiency, and an efficient numerical tool is presented in the current work to elaborate such optimized flow-control applications.

6. CONCLUSIONS AND OUTLOOK

A delay of boundary-layer transition is obtained by a single DBD actuator operated 350mm downstream of the leading edge of a flat plate subject to an adverse pressure gradient. The effect is analyzed in terms of hydrodynamic stability by obtaining averaged velocity profiles in close proximity of the DBD actuator with laser optical measurements. The velocity profiles and higher-order derivatives are inserted as boundary conditions into a linear stability solver to calculate the growth rates of modal disturbances in the linear amplification stage. The cumulative N -factor evolution shows decreased disturbance growth under the effect of flow-control forcing at various actuator thrust levels. For higher forcing magnitudes, increased stabilization of the flow is observed, leading to increasing critical Reynolds numbers.

Since extensive parameter combinations cannot be investigated in wind-tunnel experiments, a numerical procedure for the prediction of DBD flow-control effects is required. One specific finite-difference solver for the boundary-layer equations [14] is presented, incorporating a DBD force model for the simulation of laminar boundary-layer flow subjected to single or multiple DBD actuators. A setup employed for transition delay in flight [20] is numerically simulated, and application of the linear stability analysis yields excellent agreement between experimentally measured transition locations and the semi-empirical N -factor method with the commonly accepted threshold value of $N_t = 10$. The expected transition delay due to DBD operation is in the order of 2%, slightly underestimating the experimentally observed value. Although numerical studies without a thoroughly validated, physics-based DBD flow control model cannot perfectly represent all local stability properties of the flow, the conservative prediction by the chosen numerical method renders the numerical tool valuable for flow-control optimization studies.

The numerical routine enables simulation of any desirable positioning and number of DBD force fields, transcending the limitations of currently available hardware implementation. Conducting thought experiments like spatially continuous force generation, the flow-control potential can be estimated for improved actuator configurations potentially available in the near future.

ACKNOWLEDGEMENTS

This investigation has been sponsored by the Air Force Office of Scientific Research under grant FA8655-11-1-3067 and supervision by Gregg Abate. The U.S. Government is authorized to reproduce and distribute reprints for governmental purposes notwithstanding any copyright notation thereon.

REFERENCES

- [1] Johnson, G. A. and Scott, S. J., "Plasma - Aerodynamic Boundary Layer Interaction Studies," 32nd AIAA Plasmadynamics and Lasers Conference and 4th Weakly Ionized Gases Workshop, Anaheim, CA, 2001, AIAA 2001 - 3052.
- [2] Visbal, M. R., "Strategies for control of transitional and turbulent flows using plasma-based actuators," *Int. J. Comput. Fluid. Dynam.*, Vol. **24**, No. 7, 2010, pp. 237–258.
- [3] Grundmann, S. and Tropea, C., "Experimental Transition Delay Using Glow-Discharge Plasma Actuators," *Exp. Fluids*, **42**, pp. 653–657 (2007).
- [4] Seraudie, A., Vermeersch, O., and Arnal, D., "DBD Plasma actuator effect on a 2D model laminar boundary layer. Transition delay under ionic wind effect." AIAA 2011-3515, 29th AIAA Applied Aerodynamics Conference, Honolulu, Hawaii , (2011).
- [5] Quadros, R., Numerical Optimization of Boundary-Layer Control using Dielectric Barrier Discharge Plasma Actuator, Ph.D. thesis, TU Darmstadt, (2009).
- [6] Duchmann, A., Reeh, A., Quadros, R., Kriegseis, J., and Tropea, C., "Linear Stability Analysis for Manipulated Boundary-Layer Flows using Plasma Actuators," Seventh IUTAM Symposium on Laminar-Turbulent Transition, edited by G. M. L. Gladwell, R. Moreau, P. Schlatter, and D. S. Henningson, Vol. **18** of IUTAM Bookseries, Springer Netherlands, pp. 153–158 (2010).
- [7] Riherd, M. and Roy, S., "Linear Stability Analysis of a Boundary Layer with Plasma Actuators," AIAA 2012-0290, 50th AIAA Aerospace Science Meeting and Exhibition, Nashville, Tennessee, (2012).
- [8] Duchmann, A., Vieira, D., Grundmann, S., Schäfer, M., and Tropea, C., "Linear Stability Analysis of Direct Numerical Simulations of a Boundary-layer Flow Controlled by Plasma Actuators," 2nd International Conference on Computational Engineering, Darmstadt, Germany (2011).
- [9] Kriegseis, J., Schwarz, C., Duchmann, A., Grundmann, S., and Tropea, C., "PIV-based Estimation of DBD Plasma-Actuator Force terms," AIAA 2012-411. 50th AIAA Aerospace Sciences Meeting, Nashville, Tennessee, USA, (2012).
- [10] Duchmann, A., Grundmann, S., and Tropea, C., "Delay of Natural Transition with Dielectric Barrier Discharges," *Exp. Fluids*, **54**:1461 (2012)
- [11] Duchmann, A., "Boundary-Layer Stabilization with Dielectric Barrier Discharge Plasmas for Free-Flight Application," PhD thesis, TU Darmstadt, (2012). urn:nbn:de:tuda-tuprints-33513
- [12] Kriegseis, J., Performance Characterization and Quantification of Dielectric Barrier Discharge Plasma Actuators, Ph.D. thesis, TU Darmstadt (2011).
- [13] van Ingen, J. L., "A suggested semi-empirical method for the calculation of the boundary layer transition region," Tech. rep., Delft University of Technology (1956).
- [14] Köhler, M., Development and Implementation of a Method for Solving the Laminar Boundary Layer Equations in Airfoil Flows, Master thesis, TU Darmstadt (2011). urn:nbn:de:tuda-tuprints-31734
- [15] Cebeci, T. and Keller, H. B., "Shooting and parallel shooting methods for solving the Falkner-Skan boundary-layer equation," *J. Comput. Phys.*, **7**, No. 2, pp. 289–300 (1971).
- [16] Shyy, W., Jayaraman, B., and Andersson, A., "Modeling of glow discharge-induced fluid dynamics," *J. Appl. Phys.*, **92**, pp. 6434 (2002).
- [17] Roy, S., "Flow actuation using radio frequency in partially ionized collisional plasmas," *Appl. Phys. Lett.*, **86**, pp. 101502 (2005).

- [18] Singh, K. P. and Roy, S., "Force approximation for a plasma actuator operating in atmospheric air," *J. Appl. Phys.*, **103**, pp. 013305 (2008).
- [19] Maden, I., Maduta, R., Kriegseis, J., Jakirlic, S., Schwarz, C., Grundmann, S., and Tropea, C., "Experimental and computational study of the flow induced by a plasma actuator," 9th International ERCOFTAC Symposium on "Engineering Turbulence Modelling and Measurements", Thessaloniki, Greece (2012).
- [20] Duchmann, A., Simon, B., Magin, P., Tropea, C., and Grundmann, S., "In-Flight Transition Delay with DBD Plasma Actuators," 51st AIAA Aerospace Sciences Meeting, Grapevine, Texas, USA (2013).
- [21] Drela, M., "XFOIL: An Analysis and Design System for Low Reynolds Number Airfoils," Conference on Low Reynolds Number Airfoil Aerodynamics, University of Notre Dame (1989).
- [22] Arnal, D., Casalis, D., and Houdeville, R., "Practical Transition Prediction Methods: Subsonic and Transonic Flows," AVT-151 RTO AVT/VKI Lecture Series, Rhode St. Gense, Belgium (RTO-EN-AVT-151-08), 2008, ISBN 978-92-837-0900-6.
- [23] Vieira, D., Kriegseis, J., Grundmann, S., and Schäfer, M., "Numerical simulation of boundary-layer stabilization using plasma actuators," European Congress on Computational Methods in Applied Sciences and Engineering, Vienna, Austria (2012).
- [24] Fransson, J. H. M. and Alfredsson, P. H., "On the Disturbance Growth in an Asymptotic Suction Boundary Layer," *J. Fluid Mech.*, **482**, pp. 51–90 (2003).